



**HAL**  
open science

# Evaluation of Human Exposure owing to Wireless Power Transfer Systems in Electric Vehicles

Adel Razek, Lionel Pichon, Abelin Kameni, Ludovic Makong, Sahand Rasm

## ► To cite this version:

Adel Razek, Lionel Pichon, Abelin Kameni, Ludovic Makong, Sahand Rasm. Evaluation of Human Exposure owing to Wireless Power Transfer Systems in Electric Vehicles. *Athens Journal of Technology & Engineering*, 2019, 6 (4), pp.239-258. 10.30958/ajte.6-4-3 . hal-04310829

**HAL Id: hal-04310829**

**<https://cnrs.hal.science/hal-04310829>**

Submitted on 29 Nov 2023

**HAL** is a multi-disciplinary open access archive for the deposit and dissemination of scientific research documents, whether they are published or not. The documents may come from teaching and research institutions in France or abroad, or from public or private research centers.

L'archive ouverte pluridisciplinaire **HAL**, est destinée au dépôt et à la diffusion de documents scientifiques de niveau recherche, publiés ou non, émanant des établissements d'enseignement et de recherche français ou étrangers, des laboratoires publics ou privés.

## Evaluation of Human Exposure owing to Wireless Power Transfer Systems in Electric Vehicles

By Adel Razek<sup>\*</sup>, Lionel Pichon<sup>†</sup>, Abelin Kameni<sup>‡</sup>,  
Ludovic Makong<sup>§</sup> & Sahand Rasm<sup>•</sup>

*This paper presents a general overview of wireless power transfer systems (WPT) for charging batteries in electric vehicles (EV), focusing on human exposure surveys. After describing the schematics and strategies of the two WPT problems, static (stationary parking) and dynamics (road travel), we examined the problem of exposure to radiation fields attributable to WPT systems in humans and more generally living tissues. We first study how to predict these radiated fields and examined their compliance with international standards. A model used the human body derived from magnetic resonance imaging and high resolution. It was also developed a mode by numerical computations with the method of the finite elements. An exposure assessment of a characteristic wireless inductive charging system was provided to estimate the induced electromagnetic fields. We counted the worst configuration for the exposure assessment of the wireless charging system. In a second step, we studied the sensitivity of the exposure level, taking into account the uncertainty of the parameters characterizing the electromagnetic problem. Stochastic models, helped study exposure level of an inductive power transfer system. Two non-intrusive approaches were associated with a 3D finite element method to construct adequate meta-models: the Kriging and Polynomial Chaos extensions. These two techniques proved to provide powerful tools for characterizing human exposure at 85 kHz, which is a typical frequency of inductive charging of electric vehicles.*

**Keywords:** *Electric Vehicles, Wireless Power Transfer, Battery Charging, Human Exposure, Stochastic Approaches.*

### Introduction

The automotive industry is currently undergoing profound technological change in a context where environmental concerns are at the forefront. Constraints in terms of CO<sub>2</sub> emissions have pushed the manufacturers to develop a "cleaner" concept such as electric vehicles (EV). Such a vehicle currently uses a standard cable connection for charging that may include annoying and/or inconvenient items for the user. In this context, the non-contact inductive power transfer (IPT) charger is an interesting substitute.

The two essential theories that manage the IPT are the Ampere's law of 1820 and the principle of magnetic induction found by Faraday in 1831. While Ampere

---

<sup>\*</sup>Emeritus Research Director, C.N.R.S. & Honorary Professor, CentraleSupélec, GeePs, University of Paris-Saclay and Sorbonne University, France.

<sup>†</sup>Research Director, C.N.R.S., GeePs, University of Paris-Saclay and Sorbonne University, France.

<sup>‡</sup>Associated Professor, GeePs, University of Paris-Saclay and Sorbonne University, France.

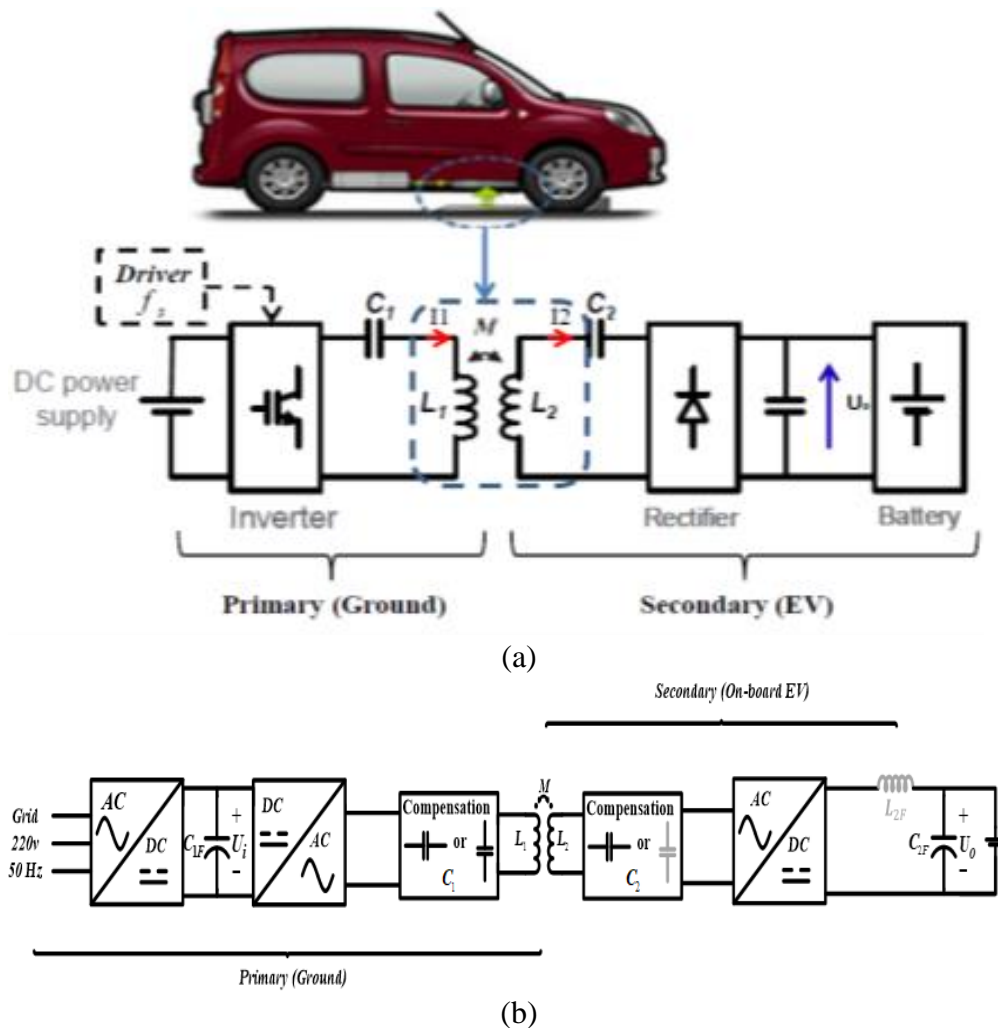
<sup>§</sup>PhD, Research Engineer, GeePs, France.

<sup>•</sup>MSc Student, GeePs, France.

showed that a current could produce a magnetic field, Faraday revealed the duality between the magnetic and the electric field demonstrating that a time-varying magnetic field can be interacting with an electrical circuit in order to induce into it an electromotive force. These two principles are allowing abundant applications commanding the development of the modern energy conversion devices. The first real improvement in the direction of IPT arrived with Tesla's studies.

Nikola Tesla (1856-1943) first introduced wireless power transfer in the 1890s (Tesla 1904), but it was only recently that this technology has been widely exploited for societal applications. In particular, the extension of resonant wireless energy technology can be used for the charging of many everyday devices. Various terms, including inductive power transfer (IPT), inductive coupling, and resonant power transfer, are generally referred as wireless power transfer (WPT). These different terms are designated to the same essential procedure - the transfer of energy from a power source to a load, without contact, through an air gap. A wireless energy transfer system consists essentially of two coils - a transmitter and a receiver.

**Figure 1.** IPT Charging System for EV: (a) System Arrangement (b) Electric Circuit



This solution offers in the case of EV simplicity of use, a speed and a decent resistance to damage of cables. The objective was to transfer energy from the ground to the vehicle (on board battery) by an inductive loop system (a transformer), as shown in Figure 1 (Ibrahim et al. 2015). This device required reaching a good performance and positioning tolerance (transmitter - receiver coupling). The coupling between the transmitter, which was placed on the ground, and the receiver, which was placed under the floor of the vehicle, was functioning through a large gap. This large space implies a high level of parasitic field near the coils, which can pose a problem of exposure to magnetic fields for passengers or persons likely to approach the vehicle during charging operations. It is therefore necessary to evaluate the level of exposure in order to comply with international safety instructions (ICNIRP 2010).

The use of wireless inductive power transfer (IPT or WPT) is becoming an effective technology for the growth of electric mobility (Cirimele et al. 2018). In addition, with the increasing number of current research attractions and the expected intensification of the practice of such wireless charging systems for electric vehicles, it is important to initiate research efforts to wireless charging systems and the human body (Ding et al. 2014).

WPT systems could be used in static, parking mode (Ibrahim 2014) or when moving the vehicle dynamically (Cirimele 2017). The dynamic mode, even more complicated in its operational control and the need for specific infrastructures, offers the possibility of overcoming the barriers represented by the heavy storage of the battery on board, the long charging time and the limited autonomy in the case of static mode. The parasitic field level near the coils due to the large air gap can be different between static and dynamic modes, and is due to the nature and operation of the coils in both cases. In addition, the constraints of field exposures differ between the two modes; however, the exposure assessment strategies are more or less similar.

Two features mainly motivate the research efforts to interact between the wireless charging systems and the human body. One has to estimate the induced electromagnetic fields in the human body at the frequency of the wireless charging system, i.e., magnetic flux density, electric field, and current density, to evaluate the potential health effects, as well as to examine the compliance with standards defined by International Commission on Non-Ionizing Radiation Protection (ICNIRP), see (ICNIRP 2010). The other aspect was to examine the impact of the input current of the wireless charging system on the radiation levels and make available the valid data for determining the extent of design liberty of IPT systems. Much research has been dedicated to the investigation of human exposure to the electromagnetic environment, such as handset antennas and the wireless resonance power system, see for example (Okoniewski and Stuchly 1996, Shiba and Higaki 2009, Christ et al. 2013). The operating frequency derived mainly from megahertz to gigahertz.

However, due to electromagnetic compatibility and energy efficiency, the IPT system for electric vehicles, generally operates in lower frequency range (from a few kilohertz to around 100 kHz). In this frequency range, exposure studies to wireless inductive charging systems have not been enough so far. Since fields

close to the IPT system can engender high fields in the body tissues of nearby humans, we need to identify the conditions under which the IPT system can demonstrate compliance with international safety guidelines (ICNIRP 2010, IEEE Standard 2005). The evaluation of exposure of human tissues to magnetic fields needs usually suitable and sufficient modeling methodologies, based on 3D computations applied for solving the electromagnetic problem involving the wireless system, the vehicle, and the human body (ie. in the vehicle or located beside), see for example (Ding et al. 2014). In this work, an assessment focuses on the electromagnetic fields induced by a representative inductive wireless charging system in the human body. Constructed MRI (Magnetic Resonance Imaging) models produced human anatomical models with high resolution compatible with the numerical approach. A 3D numerical approach providing a scientific estimate of human exposure to this system was developed. In addition, an evaluation of the electromagnetic exposure presented both normal and unfavorable configurations.

In order to assess human exposure near WPT systems in automotive applications, adequate systematic modeling methodologies have to be developed. Recently 3D computational models have been studied and applied for solving the electromagnetic problem involving the wireless system, the vehicle, and the human body in the vehicle or located beside vehicle, see (Park 2018, Cirimele et al. 2017, Cimala, et al. 2017 and Campi et al. 2017). Such full wave computational approaches give reliable results about the radiated fields around the system or induced quantities in the human body; however, this may lead to heavy computations that need to be repeated for each new configuration. A key point in such problems is that the level of exposure is highly dependent on various parameters: shape or size of coils, geometrical characteristics of the system (structural parts of the vehicle and shielding plates), materials properties (ferrites and chassis of vehicle), possible misalignment between transmitter and receiver while charging, and position of the human body. Moreover, some uncertainty can affect each physical or geometrical parameter. Therefore, during the design of the IPT system, the consideration of level of exposure cannot only rely on deterministic full 3-D solvers. In this situation, the introduction of stochastic tools allows to deal with the variability of all the parameters which are describing the electromagnetic problem. Such approaches can be very efficient in the framework of the determination of specific rate absorption (SAR) in biological tissues due to mobile phones at microwave frequencies.

The first objective of this article was to present a general overview of wireless energy transfer systems in electric vehicles, focusing on human exposure surveys. After having illustrated the problems and strategies of the two WPT categories, static (stationary parking), see for example (Ibrahim et al. 2015) and dynamic (road travel), see for example (Cirimele et al. 2016), we examine the problem of exposure to radiation fields attributable to WPT systems in humans and more generally in living tissues.

In the second objective of this work, we studied the sensitivity of the exposure level taking into account the uncertainty of the parameters characterizing the electromagnetic problem. Due to this aim, we compared different stochastic methods during the investigation of the compliance of IPT systems with

international standards, regarding the human exposure. We focused on so-called non-intrusive methods that use 3D finite element computations with a limited set of realizations. Kriging and Polynomial chaos have already shown their interest in numerical dosimetry and optimization in the case of extremely low frequency (50 Hz), see (Lebensztajn et al. 2004 and Gaignaire et al. 2012) or wave propagation problems, see (Voyer et al. 2008 and Kersaudy et al. 2014). In this paper, the two techniques provided powerful tools to characterize the human exposure at 85 kHz, which is a typical frequency for inductive charging of electrical vehicles.

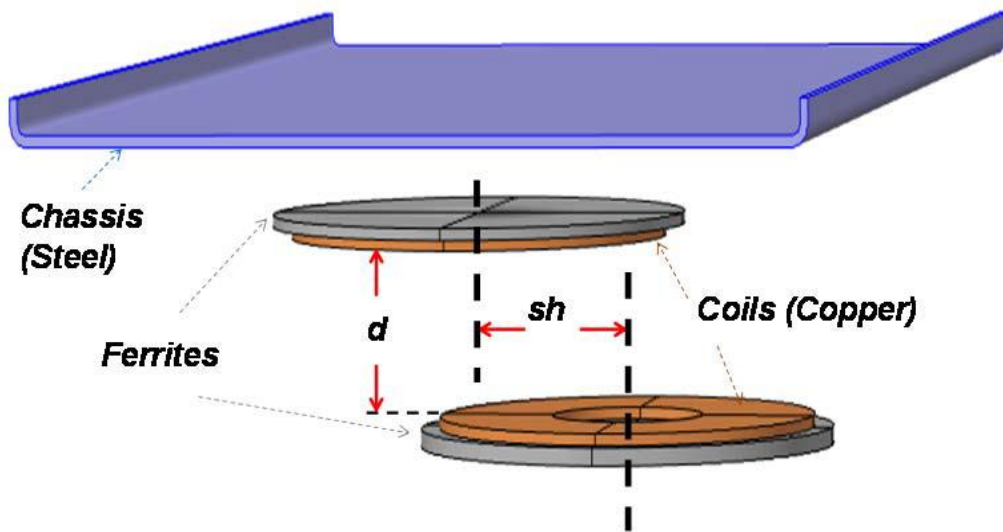
## Wireless Power Transfer WPT

### *Static WPT*

An IPT system for charging battery of a static EV, is represented in Figure 1. It is composed of an electrical source, a load (battery) and in between an inductive coupler transformer (ICT) with shielded coils. Planar parallel axes shielded coils could produce concerning the ICT structure, one of the most proficient magnetic flux transfers. In such a situation, the energy transfer functions overall receiver surface and shielding that is used to improve the mutual inductance ( $M$ ) by increasing the magnetic flux between the two coils. The shielding is accomplished by a magnetic almost none conducting material and ferrite is usually used.

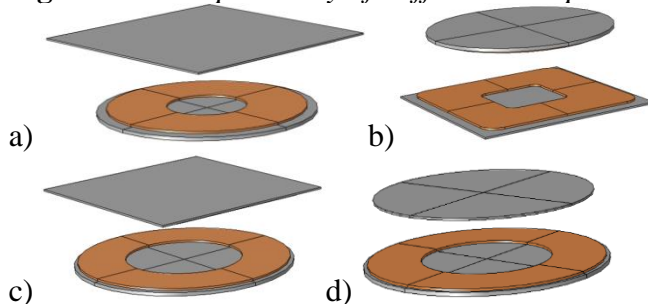
The complete scheme is composed of two major parts: the ICT that allows the wireless transfer through the magnetic induction and that ensures a galvanic insulation between the source and the load. The second feature comprises the capacitive compensations and the power electronics connected to ICT, which manages the arrangement to operate at resonance. The whole system practices IPT system. Between the grid and the ICT, there are two conversion steps: grid low frequency AC to DC, and DC to AC high frequency. These conversions allow regulating the power quantity by controlling the input voltage and the frequency. Between the ICT and the battery, a finishing conversion from high frequency AC to DC permits granting energy to the battery. The air gap of the ICT is large and then the coupling is weak. Therefore, administering the high reactive power is required in order to reach the required transferred power, and the use of resonant elements in both sides of the ICT is indispensable as compensation to guarantee good efficiency. In addition, control of the output parameters at the load side is needed in order to monitor the battery charging profile and to insure its protection.

A structure of the ICT coupler is shown in Figure 2. It consists of a transmitter coil, a receiver coil and two ferrites plates that completely cover the coils. The design included a steel plate that represented the EV chassis. The two ICT coils with their ferrites (pads) are identical with an air gap distance ( $d$ ), and axes shift ( $sh$ ), in the case of Figure 2, which corresponds to the EV position on the ground. In societal applications situation, the two coils (and generally pads) forms may be different depending on constructors of EVs and IPTs. Therefore, in such case, we need to perform an interoperability analysis (Ibrahim et al. 2016).

**Figure 2.** 3-D Structure of an ICT with Shielding, Simple EV Chassis

Generally, we can use 3D electromagnetic field computations, for example the finite elements method (FEM) simulations, for the ICT considering the whole structure of the IPT (see Figure 2) for the determination of its mutual coupling and inductances (see Figure 1). The effect of shielding using coil-closed ferrites to reduce the leakage fields and to border the penetration of the field within the vehicle required consideration in such simulations. Moreover, in the structure of the IPT system the EV chassis was modeled (Ibrahim 2014). In fact, the presence of the EV chassis modifies the field values, and hence the matching inductances of the power system and the electromagnetic compatibility (EMC) radiation level. After deducing the mutual coupling and inductances of the ICT, accounting for the IPT structure from the field values, an electrical circuit model of the whole system including the resonance topology was established (Figure 1).

As mentioned before, in practice we need an interoperability analysis concerning the forms and surfaces of the pads (coils/ferrites) of ground regarding those of EVs. This analysis concerns the position of EV pad in the vehicle (middle or backend), the tolerance to positioning of vehicle, the human exposure recommendations, the efficiency, the sizes of power components of the IPT. A detailed analysis of this question is presented in Ibrahim et al. (2016). Figure 3 shows different examples of compatible pads.

**Figure 3.** Interoperability of Different Compatible Prototypes

*Dynamic WPT*

In the last section, we discussed static IPT. Such technology indicated as static, when the vehicle parked or motionless during charging, will likely replace the wired systems. However, the absence of mechanical stresses, in the course of charging, suggests the possibility of using the inductive transfer when moving the vehicle that uses the dynamic IPT. In such a case, the receiver of the IPT installed on the bottom of the vehicle will move over successive transmitters fixed on the ground infrastructure (Figure 4).

The putting in place of dynamic IPT systems in the road infrastructure will abolish the need for charging stops and, in the short term, this appliance could result in a significant reduction in the size of the battery installed on-board. The successful demonstration of the feasibility of this technology may indicate a concrete approach to improve the acceptance of electric mobility and to solve the most critical aspects of the use of electric vehicles.

An important technical problem for the dynamic IPT is the identification of the vehicle when it approaches a transmitter and the management of the passage between the successive transmitters. Moreover, as in the case of static IPT, there is the aspect of protection against exposure to magnetic fields generated in the dynamic IPT.

**Figure 4.** *Dynamic IPT*

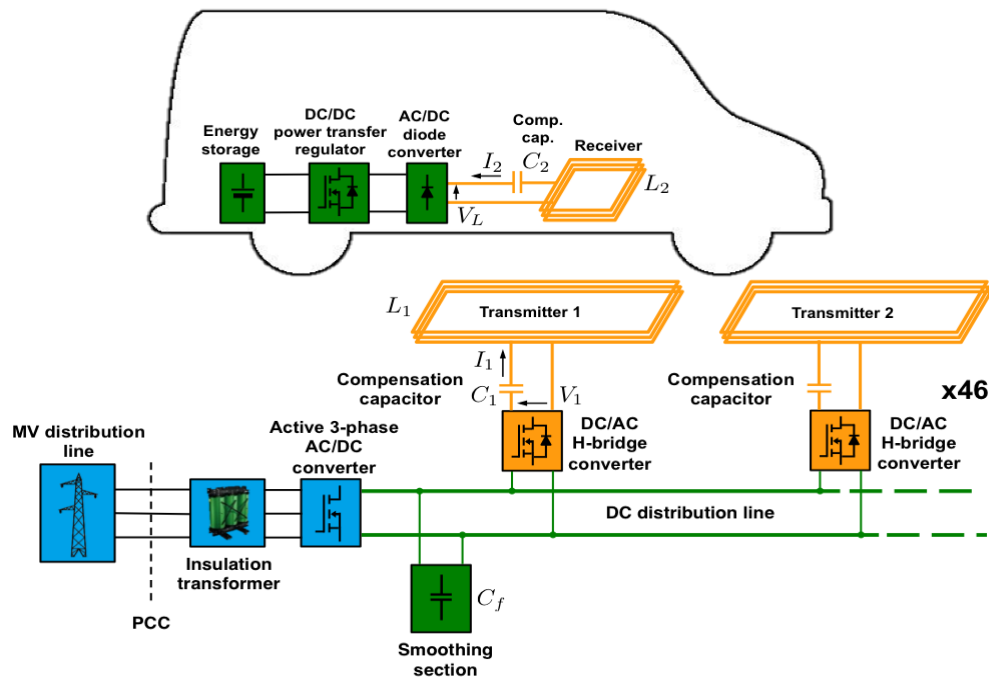


Finally, there is the vast quantity of defies represented by all the aspects related to the establishment of the road infrastructure. In particular, the insertion of the emitting portion in the pavement, the choice of material for the coating, the management of the rainwater, the need to communicate with the relating management infrastructure.

Different recent works are concerned by these aspects, see for example (Cirimele 2017) – Figure 5.



**Figure 5.** Scheme of the General Architecture of the IPT System Developed for On-the-Road Prototype (Cirimele, 2017)



## Human Exposure

As mentioned before, the large space between the two coils of IPT in either of static or dynamic cases implies a high level of parasitic field near the coils. This situation posed a problem of exposure to magnetic fields for passengers or persons likely to approach the vehicle during charging operations. Therefore, to comply with societal health safety, it was necessary to evaluate the level of exposure concerning the international safety instructions (ICNIRP 2010).

### *Prediction of Radiated Fields*

The evaluation of exposure of living tissues to magnetic fields needs generally adequate modeling methodologies based on 3D computations applied for solving the electromagnetic problem involving the wireless system, the vehicle and the human body (in the vehicle or beside vehicle). In such computations, the considered human body model is very important. The most critical aspects governing the choice of such a model are fidelity to physical biological characteristics of realistic situation and the adaptability to the used computational methodology. There are considerable research efforts devoted to the construction of human body models. Usually, the computations of electromagnetic fields in human body require computer-adapted models of the human body and a comprehensive information of the dielectric properties of human tissues for a given frequency. These models are of two categories, homogeneous and non-

homogeneous. For homogeneous ones, the dielectric properties of the human body are generally attributed to a 2/3 equivalent muscle model (Harris et al 2011). For non-homogeneous human models, ghost models of layered tissue are founded on magnetic resonance imaging (MRI), computed tomography and digital imaging techniques, offering precision of tissue shape to the nearest millimeter (Gjonaj et al. 2002, and Steiner et al 2006). The dielectric properties of biological tissues are described in Hasgall et al. (2012) and Gabriel et al. (1996). A comprehensive description of the accessible measurement data for dielectric permittivity and electrical conductivity for any specified frequency was specified by Gabriel et al. (1996).

### *Conformity with International Standards*

The fields close to the IPT systems can produce high fields in the body tissues of nearby humans and we need to characterize the conditions under which the IPT system can validate agreement with international safety guidelines (ICNIRP 2010, IEEE Standard 2005). The evaluation of exposure of human tissues to magnetic fields needs suitable and complete modeling methodologies based on 3-D computations for solving the electromagnetic problem involving the wireless system, the vehicle and the human body (Ding et al. 2014).

**Figure 6.** *Vertical Body and Wireless Inductive Charging System*

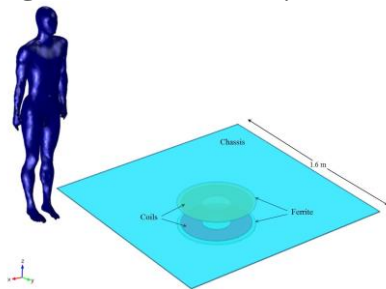
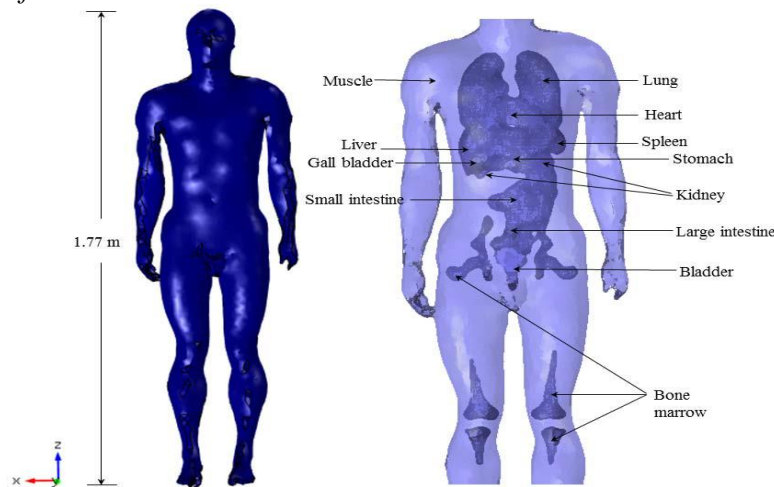


**Figure 7.** *Anatomical whole Body Model and its Different Tissues and Organs of Interest*



The configurations studied involving the human body, the IPT coils with ferrites and the chassis shown schematically in Figure 6. The study considers the two cases of vertical and horizontal positions of human body. The high-resolution human anatomical model compatible with the numerical approach constructed from human MRI models, as shown in Figure 7. Examples of results obtained in (Ding et al. 2014) are shown in Figures 8 and 9 corresponding to positions: vertical and horizontal (laying the ground) respectively. The obtained results confirm the agreement with international safety guidelines ( $27 \mu\text{T}$  for the magnetic induction B and  $4.05 \text{ V/m}$  for electric field E).

**Figure 8.** Distribution of Induced Fields inside the Anatomical Human Body for the Configuration of Figure 6. (a) Magnitude of Magnetic Flux Density B (T), (b) Magnitude of Electric E-field (V/m) (Ding et al 2014)

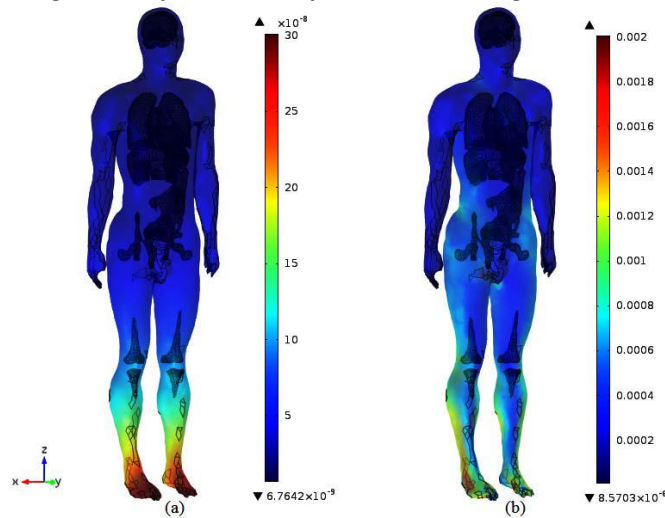
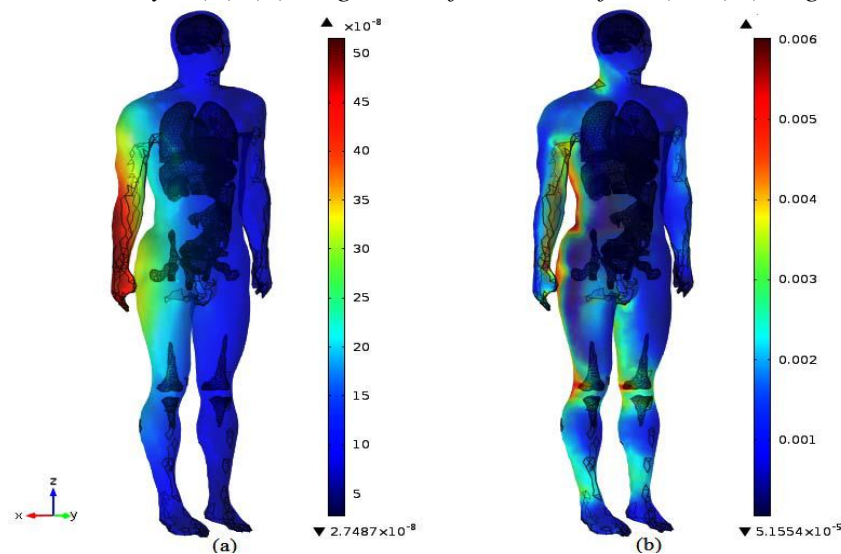


**Figure 9.** Distribution of Induced Fields inside the Anatomical Human Body for the Configuration of Horizontal, Ground Lying Body. (a) Magnitude of Magnetic Flux Density B (T), (b) Magnitude of Electric E-field (V/m). (Ding et al 2014)



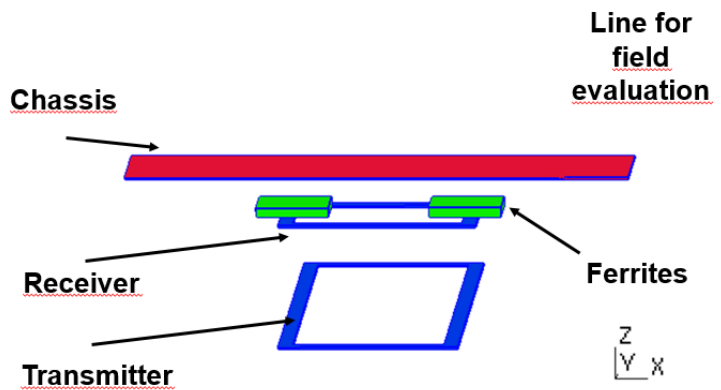
## Non-Intrusive Stochastic Approaches

As mentioned before, the objective of this work was to compare different stochastic methods when investigating the compliance of IPT systems with international standards regarding the human exposure. We focused on so-called non-intrusive methods that use 3-D finite element computations with a limited set of realizations.

### Wireless Power Configuration

The structure model of the system considered in this work contains two rectangular coils (transmitter and receiver), and two ferrites plates (Cirimele, 2017). The design also includes a steel plate that represents the chassis of the electric vehicle (Figure 10).

**Figure 10.** Studied Configuration of Wireless Transfer System (Cirimele, 2017)



The dimensions of the system are shown in Table 1.

**Table 1.** Dimensions of Figure 10

	Width (m)	Length (m)
Transmitter	0.5	1.5
Receiver	0.525	0.3
Ferrites	0.2	0.25
Chassis	1.5	0.5

The relative permeability of ferrites is 2000. Each coil has 10 turns. A 3-D vector potential formulation has solved the magneto-dynamic problem. This system has been designed for dynamic charging but in the present work, only a static charging scenario was considered. The power electronics controls and keeps the *rms* value of the current in the transmitter at 36 A, and the current in the receiver at 75 A, respectively. The electromagnetic quantities were evaluated along the vertical line located at 1m from the axis of the transmitter (Figure 10).

### Stochastic Models

In this work investigated two non-intrusive stochastic methods: Kriging and Polynomial Chaos.

#### Kriging

Kriging is a stochastic interpolation algorithm that assumes that the model output  $M(x)$  is a realization of a Gaussian process indexed by the inputs  $x$ . A Kriging meta-model was described by the following equation:

$$M(x) \sim M^K(x) = \beta^T f(x) + \sigma^2 Z(x, \omega) \quad (1)$$

The first term in (1), is the mean value of the Gaussian process (trend) and it consists of the regression coefficients  $\beta_j$  ( $j = 1 \dots P$ ) and the base functions  $f_j$  ( $j = 1, \dots, P$ ). The second term in consists of  $\sigma^2$ , the (constant) variance of the Gaussian process and  $Z(x, \omega)$ , a zero mean, unit variance, stationary Gaussian process. The underlying probability space was represented by  $\omega$  and was defined in terms of a correlation function  $R$  and its hyper-parameters  $\theta$ . The correlation function  $R = R(x; x_0; \theta)$  described the correlation between two samples of the input space, *e.g.*  $x$  and  $x_0$  and depends on the hyper- parameters  $\theta$ . In the context of meta-modelling, it is of interest to calculate a prediction  $M^K(x)$  for a new point  $x$ , given  $X = (x_1 \dots x_n)$ , the experimental design, and  $y = (y_1 = M(x_1), \dots, = M(x_n))$ , the corresponding (noise-free) model responses. A Kriging meta-model (Kriging predictor) provided such predictions based on the Gaussian properties of the process.

#### Polynomial Chaos Expansion

The polynomial chaos is a spectral method and consists in the approximation of the system output in a suitable finite-dimensional basis  $\Psi(X)$  made of orthogonal polynomials. A truncation of this polynomial expansion can be as follows:

$$M(x) \sim M^{PC}(x) = \sum_0^{P-1} \alpha_j \Psi_j(X) \quad (2)$$

where  $M(x)$  is the system output,  $X$  is the random input vector made of the input parameters  $x_i$ ,  $\Psi_j$  are the multivariate polynomials belonging to  $\Psi(X)$ ,  $\alpha_j$  are the coefficients to be estimated,  $\varepsilon$  is the error of truncation, and  $P$  is the size of the polynomial basis  $\Psi(X)$ . Each multivariate polynomial  $\Psi_j$  was built as a tensor product of univariate polynomials orthogonal with respect to the probability density function of each input parameter  $x_i$ . In the present work, the value of  $P$  around 15 provided reliable results. Here, inputs used Gaussian distributions, and the corresponding polynomial families were the Hermite polynomials families.

The coefficients in (2) are estimated from spectral projections or least-square regressions.

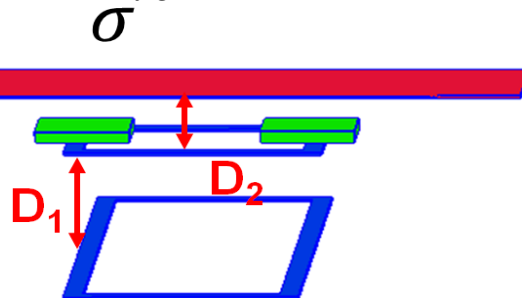
## Results

Marelli and Sudret (2014) developed the two stochastic models described above and used in this paper. The models were proposed in the framework for uncertainty quantification in UQLab ([www.uqlab.com](http://www.uqlab.com)) and are freely available. Configurations were applied in the two previous approaches (refer to Figure 10) to check the compliance regarding the references levels of radiated magnetic field. For the frequency of interest (85 kHz), the maximum admissible value of the magnetic flux density was 27  $\mu\text{T}$  according to the ICNIRP Guidelines (ICNIRP 2010).

### First Configuration

In a first example, investigation of uncertainties included three major parameters: the conductivity of the chassis  $\sigma$ , the distance between the two coils  $D_1$  and the distance between the secondary coil (receiver) and the chassis  $D_2$  (Figure 11).

**Figure 11.** Studied Configuration and Relevant Parameters



The range of variation, mean, and standard deviation of the parameters are shown in Table 2. Two bounds took into account different kinds of steel material for the conductivity. The bounds for the two distances  $D_1$  and  $D_2$  exceed standards values of existing systems in order to evaluate the worst cases. The 3D finite element mesh includes between  $10^5$  and  $3.10^5$  elements depending on the geometrical configuration of the system. The method used first order nodal elements.

**Table 2.** Parameters of the Electromagnetic Problem

Parame-ter	Min	Max	Mean	Standard Variation
$\sigma$ (S/m)	$10^6$	$5.10^6$	$3.10^6$	$10^6$
$D_1$ (m)	0.2	0.6	0.4	0.05
$D_2$ (m)	0.1	0.5	0.3	0.01

A total number of 30 computations performed by FEM based on a Gaussian distribution of samples over the whole range of variations in order to check the efficiency of the two meta-models. In the first case, only three FEM computations (learning samples) were used to build the meta-models. The other 27 computations have been used as a validation of the meta-model. Figure 12 shows the magnitude of the magnetic field density on the evaluation line obtained by Kriging and Polynomial expansion when the values of the parameters are  $\sigma = 1.89 \cdot 10^6$  S/m;  $D_1 = 0.405$  m;  $D_2 = 0.312$  m. It clearly appears in this case with only three samples that the agreement between the results from the polynomial expansion was very close to the finite element predictions. The accuracy was significantly better than that provided by Kriging. Figure 13 underlines the differences between the results obtained by finite elements (horizontal axis) and by the meta-models (vertical axis) when considering the 27 finite element computations as validation.

**Figure 12.** Variation of Magnetic Flux Density Predicted by Meta-Models in the Case of the Three Learning Samples

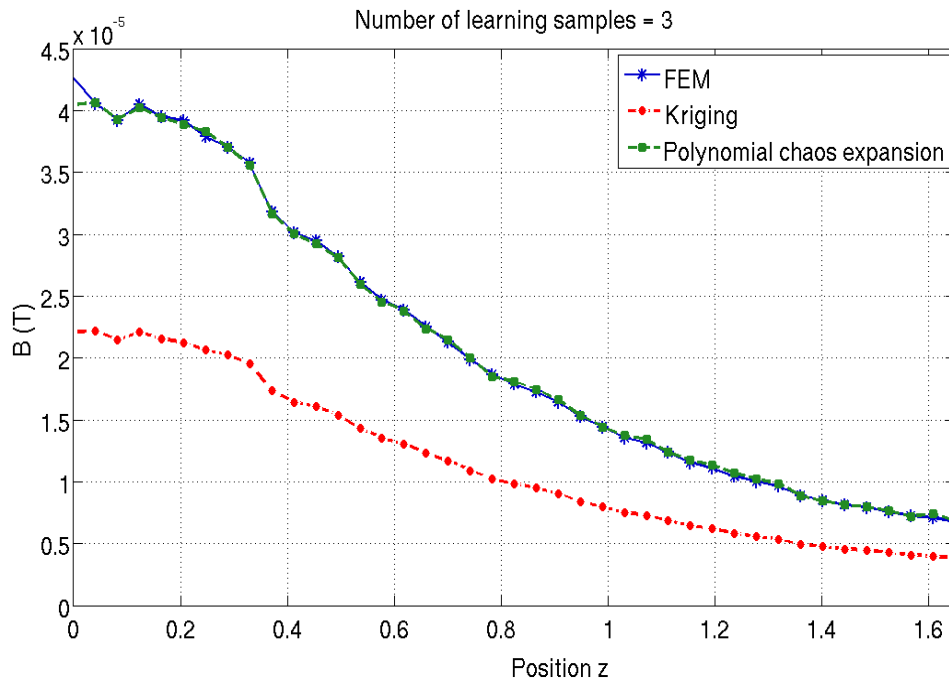


**Figure 13.** Differences between Finite Element Results and Meta-Modeling Results in the Case of the Three Learning Samples

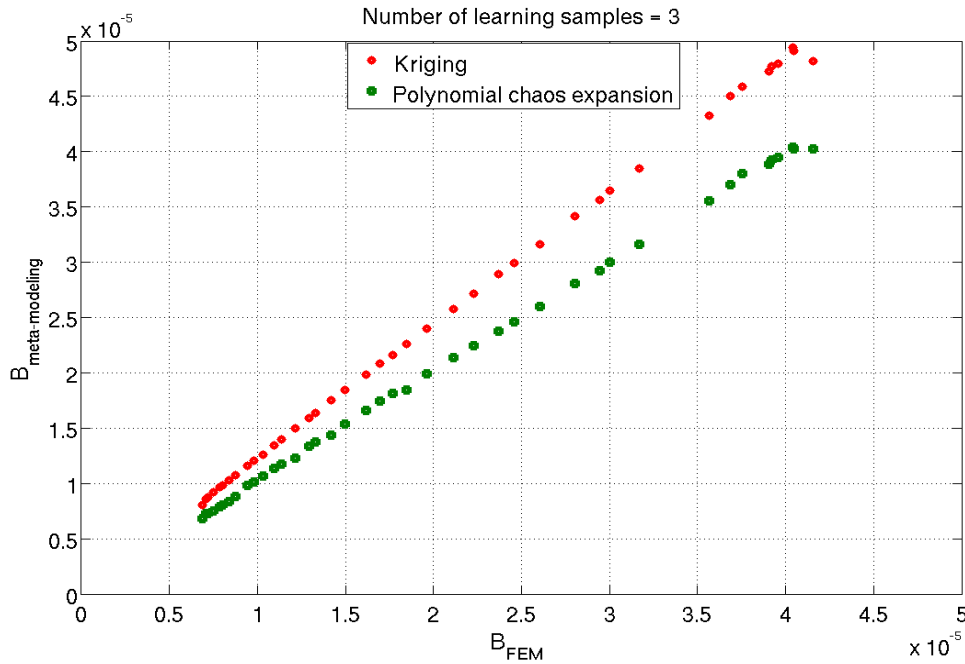
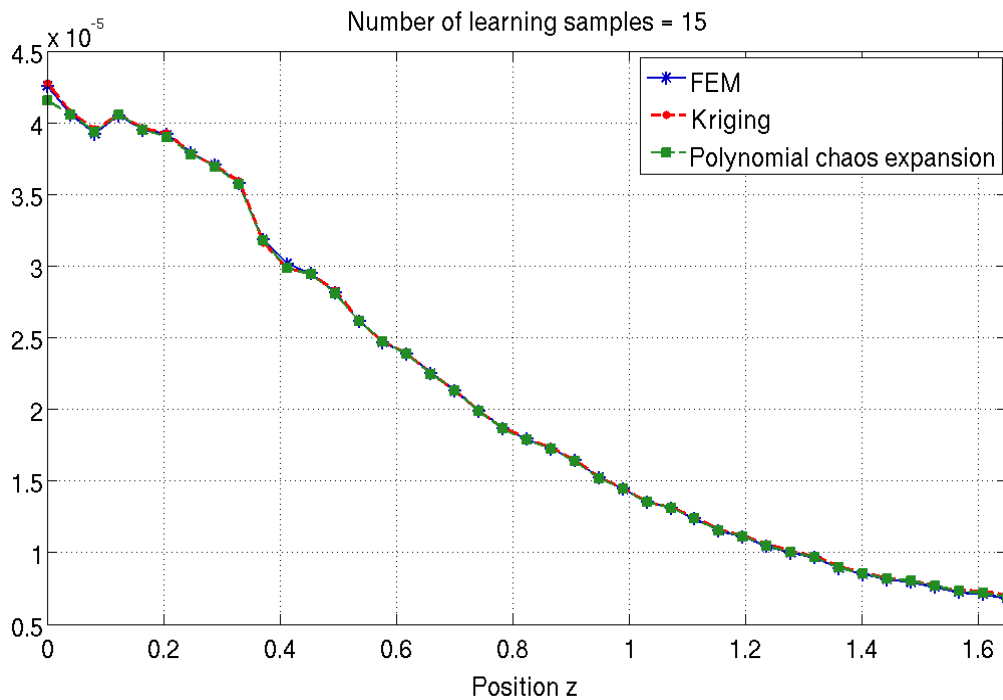


**Figure 14.** Variation of Magnetic Flux Density Predicted by Meta-Models in the Case of the 15 Learning Samples

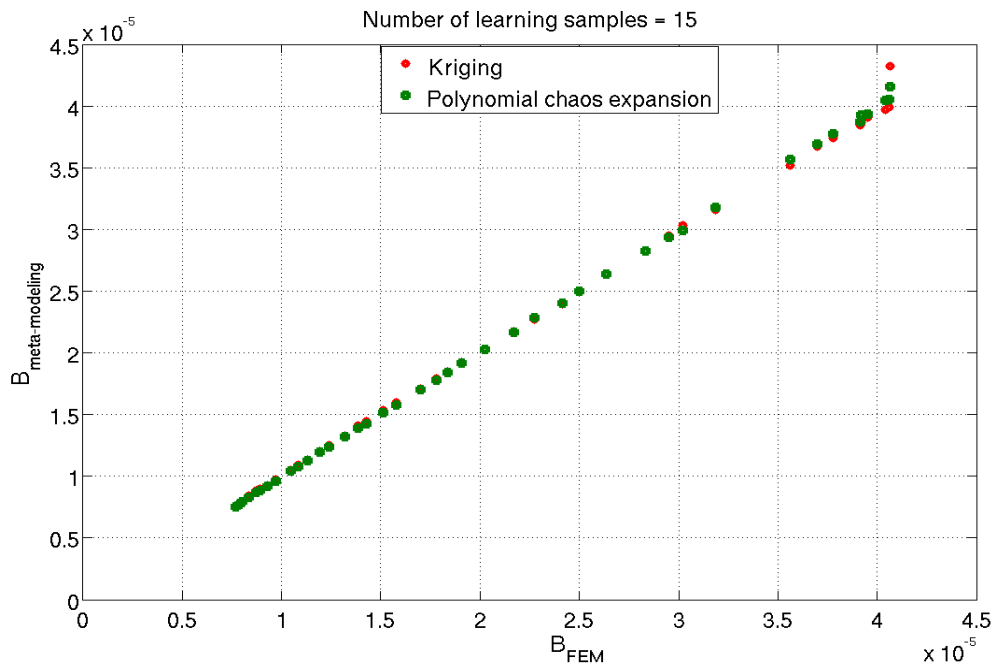


In a second case, 15 FEM computations were used as learning samples. The other 15 computations were used for the validation. Figure 14 shows that the agreement between the results from the two meta-models was very good. This can

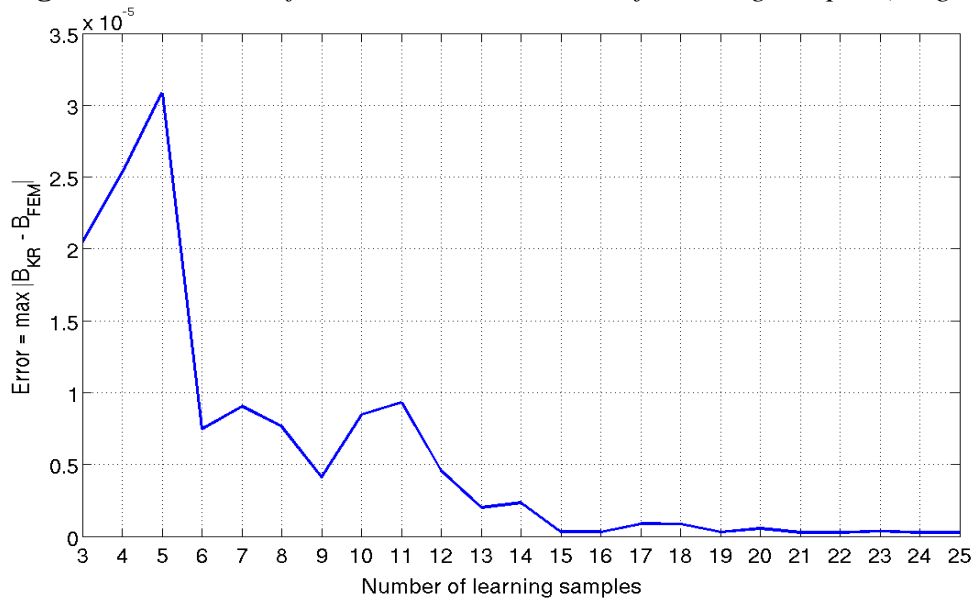


also be noted on Figure 15 where were plotted the differences between the results obtained by finite elements (horizontal axis) and by the meta-models (vertical axis) when considering the 15 finite element computations as a validation. The accuracy of each meta-model can be observed on Figures 16 and 17 showed the maximum error obtained along the evaluation line versus the number of learning samples. High errors for high values of flux density were obtained but it was worth noting that this error was decreased significantly with Kriging if the number of learning samples was greater than 10.

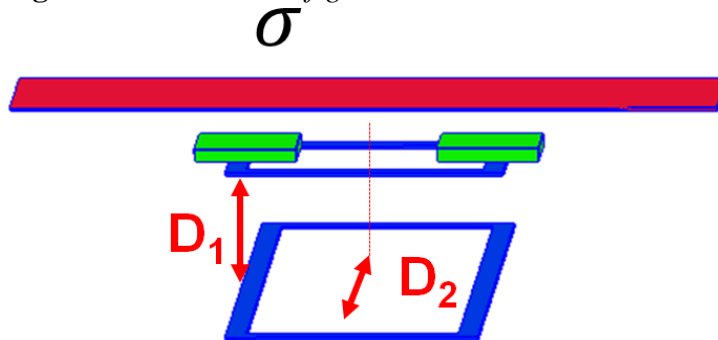
**Figure 15.** Differences between Finite Element Results and Meta-Modeling Results in the Case of the 15 Learning Samples



Regarding the computational time needed by the meta-models, Kriging required two or three times faster than Polynomial chaos expansion depending on the number of learning samples. Whatever the meta-model and the number of learning samples this computational time remains negligible compared to the FEM calculation for all the samples.

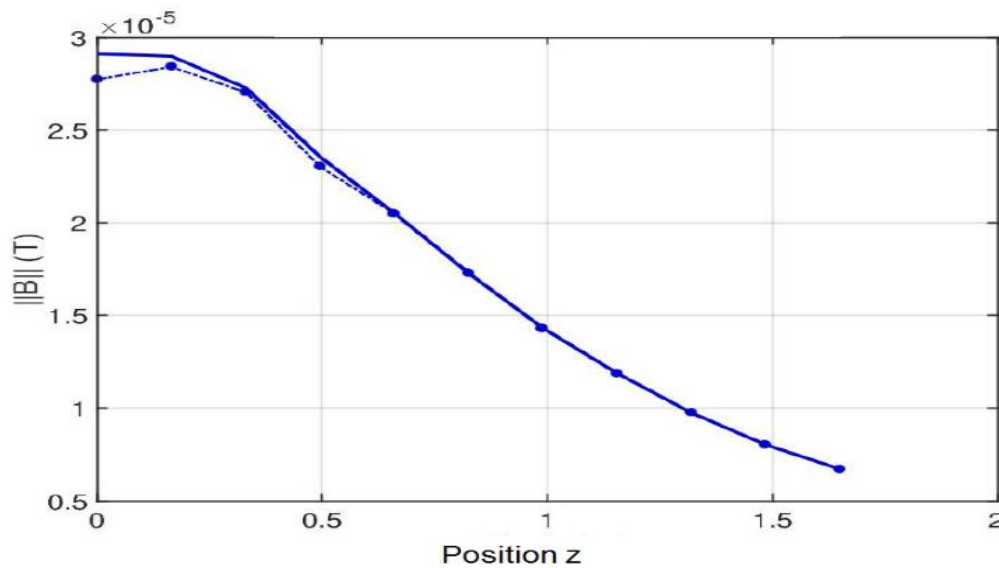
**Figure 16.** Variation of Error versus the Number of Learning Samples (Kriging)*Second Configuration*

In this second configuration, the two parameters  $\sigma$  and  $D_1$  were the same as those shown in Figure 11; however,  $D_2$  was the distance between the two axes of the coils. This configuration may appear in case of large misalignment or if the receiver is located in the rear of the vehicle. The range of variation, mean and standard deviation for the parameters are shown in Table 3. Figure 18 illustrates the mean value obtained by Kriging along the evaluation line.

**Figure 17.** Studied Configuration and Relevant Parameters**Table 3.** Parameters of the Electromagnetic Problem

Parameter	Min	Max	Mean	Standard Variation
$\sigma$ (S/m)	$10^6$	$5 \cdot 10^6$	$3 \cdot 10^6$	$10^6$
$D_1$ (m)	0.2	0.6	0.4	0.05
$D_2$ (m)	-1.5	1.5	0.	0.1

**Figure 18.** Mean Value of the Magnetic Flux Density obtained by Kriging (Dots) and by Finite Elements (Continuous Line)



## Conclusions

In the first part of this paper we presented a general overview of wireless power transfer systems (WPT) for charging batteries in electric vehicles (EV), focusing on human exposure surveys. After describing the schematics and strategies of the two WPT problems, static (stationary parking) and dynamics (road travel), we examined the problem of exposure to radiation fields attributable to WPT systems in humans living tissues. We reviewed how to predict these radiated fields and examined their compliance with international standards.

In the second part of the paper, predictions of radiated magnetic field have been obtained from two non-intrusive stochastic models in case of a simplified but there is also realistic wireless power transfer system for electric vehicle. Kriging and Polynomial chaos expansions provided efficient meta-models to take into account uncertainties of different physical or geometrical parameters. From the work, it comes out that Kriging allowed a faster prediction than a polynomial chaos expansion. If the number of learning samples was sufficient, Kriging can be used as an efficient predictor to check if reference levels fit the guidelines for human exposure. The work has to be extended the investigation of configurations that are more complex with a detailed anatomical human body model located in the vehicle or beside.

## References

- Tesla N (1904) The Transmission of Electrical Energy without Wires. *Electrical World and Engineer* 1: 21-24.
- Ibrahim M, Bernard L, Pichon L, Razek A, Houivet J, Cayol O (2015) Advanced Modeling of a 2-Kw Series-series Resonating Inductive Charger for real Electric Vehicle. *IEEE Transactions on Vehicular Technology* 64 (2): 421-430.
- ICNIRP: International Commission on Non-Ionizing Radiation Protection (2010) Guidelines for Limiting Exposure to time-Varying Electric, Magnetic, and Electromagnetic Fields (1 Hz to 100 kHz). *Health Physics* 99(6): 818-836.
- Cirimele V, Diana M, Freschi F, Mitolo M (2018) Inductive Power Transfer for Automotive Applications: State-of-the-Art and Future Trends. *IEEE Transactions on Industry Applications* 54(5): 4069.
- Ding PP, Bernard L, Pichon L, Razek A (2014) Evaluation of Electromagnetic Fields in Human Body Exposed to Wireless Inductive Charging System. *IEEE Transactions on Magnetics* 50(2): 1037-1040.
- Ibrahim M (2014) *Wireless Inductive Charging for Electrical Vehicles: Electromagnetic Modelling and Interoperability Analysis*. PhD Thesis, University of Paris-Sud.
- Cirimele V (2017) *Design and Integration of a Dynamic IPT System for Automotive Applications*. PhD Thesis, Politecnico di Torino and Université Paris-Saclay (GeePs).
- Okoniewski M, Stuchly MA (1996) A Study of the Handset Antenna and Human Body Interaction. *IEEE Transactions on Microwave Theory and Techniques* 44(10): 1855-1864.
- Shiba K, Higaki N (2009) Analysis of SAR and Current Density in Human Tissue Surrounding an Energy Transmitting Coil for a Wireless Capsule Endoscope. *20<sup>th</sup> International Zurich Symposium on Electromagnetic Compatibility*.
- Christ A, Douglas MG, Roman JM, Cooper EB, Sample AP, Waters BH, Smith JR, Kuster N (2013) Evaluation of Wireless Resonant Power Transfer Systems with Human Electromagnetic Exposure Limits. *IEEE Transactions on Electromagnetic Compatibility* 55 (2): 265-274.
- IEEE Standards (2005) *IEEE Standard for Safety Levels with respect to Human Exposure to Radio Frequency Electromagnetic Fields, 3 kHz to 300 GHz*. Retrieved from <https://bit.ly/2LmeA2q>.
- Park S (2018) Evaluation of Electromagnetic Exposure during 85 kHz Wireless Power Transfer for Electric Vehicles. *IEEE Transactions on Magnetics* 53(1): 1-8.
- Cirimele V, Freschi F, Giaccone L, Pichon L, Repetto M (2017) Human Exposure Assessment in Dynamic Inductive Power Transfer for Automotive Applications. *IEEE Transactions on Magnetics* 53(6): 1-4.
- Cimala C, Clemens M, Streckert J, Schmuelling B (2017) Simulation of Inductive Power Transfer Systems Exposing a Human Body with a Coupled Scaled-Frequency Approach. *IEEE Transactions on Magnetics* 53(6): 1-1.
- Campi T, Cruciani S, Maradei F, Feliziani M (2017) Near Field Reduction in a Wireless Power Transfer System using LCC compensation. *IEEE Transactions on Electromagnetic Compatibility* 59(2): 686-694.
- Cirimele V, Ruffo R, Guglielmi P, Khalilian M (2016) A Coupled Mechanical-Electrical Simulator for the Operational Requirements Estimation in a Dynamic IPT System for Electric Vehicles. *2016 IEEE Wireless Power Transfer Conference (WPTC)*: 1-4.
- Lebensztajn L, Marretto CAR, Caldora Costa M, Coulomb JL (2004) Kriging: A Useful Tool for Electromagnetic Device Optimization. *IEEE Transactions on Magnetics* 40(2): 1196-1199.

- Gaignaire R, Scorretti R, Sabariego RV, Geuzaine C (2012) Stochastic Uncertainty Quantification of Eddy Currents in the Human Body by Polynomial Chaos Decomposition. *IEEE Transactions on Magnetics* 48(2): 451-454.
- Voyer D, Musy F, Nicolas L, Perrussel R (2008) Probabilistic Methods Applied to 2D Electromagnetic Numerical Dosimetry. *COMPEL* 27(3): 651-667.
- Kersaudy P, Mostarshedi S, Sudret B, Picon O, Wiart J (2014) Stochastic Analysis of Scattered Field by Building Facades Using Polynomial Chaos. *IEEE Transactions on Antennas and Propagation* 62(12): 6382-6392.
- Ibrahim M, Bernard L, Pichon L, Laboure E, Razek A, Cayol O, Ladas D, Irving J (2016) Inductive Charger for Electric Vehicle: Advanced Modeling and Interoperability Analysis. *IEEE Transactions on Power Electronics* 31(12): 8096-8114.
- Harris LR, Zhadobov M, Chahat N, Sauleau R (2011) Electromagnetic Dosimetry for Adult and Child Models within a Car: Multi-Exposure Scenarios. *International Journal of Microwave and Wireless Technologies* 3(6): 707-715.
- Gjonaj E, Bartsch M, Clemens M, Schupp S, Weiland T (2002) High-Resolution Human Anatomy Models for Advanced Electromagnetic Field Computations. *IEEE Transactions on Magnetics* 38(2): 357-360.
- Steiner T, De Gerssem H, Clemens M, Weiland T (2006) Local Grid Refinement for low-Frequency Current Computations in 3-D Human Anatomy Models. *IEEE Transactions on Magnetics* 42(4): 1371-1374.
- Hasgall P, Neufeld E, Gosselin MC, Kingenböck A, Kuster N (2012). *IT'IS Database for Thermal and Electromagnetic Parameters of Biological Tissues*. Retrieved from: <https://bit.ly/30KwoL9>.
- Gabriel C, Gabriel S, Corthout E (1996) The Dielectric Properties of Biological Tissues: II. Measurements in the Frequency Range 10 Hz to 20 GHz," *Physics in Medicine & Biology* 41(11): 2251-2269.
- Marelli S, Sudret B (2014) UQLab: A Framework for Uncertainty Quantification in Matlab. *2<sup>nd</sup> International Conference on Vulnerability, Risk Analysis and Management (ICVRAM2014)*.